Journal of Peptide Science, Vol. 1, 251–265 (1995)

Conformational Studies on Synthetic Peptides Reproducing the Dibasic Processing Site of Pro-ocytocin–Neurophysin

CARLO DI BELLO[1], MARIO SIMONETTI[1], MONICA DETTIN[1], LIVIO PAOLILLO[2], GABRIELLA D'AURIA[2], LUCIA FALCIGNO[2], MICHELE SAVIANO[2], ANGELO SCATTURIN[3], GIANNI VERTUANI[3] and PAUL COHEN[4]

[1] Institute of Industrial Chemistry, University of Padova, Italy
[2] Department of Chemistry, University of Napoli, Italy
[3] Department of Pharmaceutical Chemistry, University of Ferrara, Italy
[4] Laboratoire de Biochimie des Signaux Régulateurs Cellulaires et Moléculaires, P. et M. Curie University, Paris, France

Received 28 November 1994
Accepted 24 January 1995

Abstract: Synthetic peptides reproducing the proteolytic processing site of pro-ocytocin were studied by different spectroscopic techniques, including circular dichroism, Fourier transform infrared absorption, and mono and bidimensional nuclear magnetic resonance, in order to ascertain the possible role of three-dimensional structure in the recognition process by maturation enzymes. Experimental results were compared with energy minimization calculations and suggest that: (i) the region situated on the N-terminus of the Lys-Arg doublet may form a β-turn; (ii) the sequential organization of the residues participating in the β-turn determines the privileged relative orientation of the basic amino acid sidechains and the subtype of turn; and (iii) the peptide segment situated on the C-terminal side of the dibasic doublet may assume a helix arrangement. These findings, in spite of the limitations connected to the flexibility of linear peptides, seem to substantiate the hypothesis that structural motifs around the cleavage site could be important for recognition and processing. However, a straightforward correlation between details of the secondary structure and the *in vitro* reactivity toward a putative convertase is not yet possible.

Keywords: Hormone biosynthesis; ocytocin; prohormone; proteolytic processing; β-turn

Abbreviations

Abbreviations used for amino acids and peptides follow the Recommendations of the IUPAC–IUB Commission of Biochemical Nomenclature (1984) *Eur. J. Biochem, 138*, 9–37. The following additional abbreviations are used: 2D, two-dimensional; ACN, acetonitrile; CD, circular dichroism; COSY, double quantum filtered correlated spectroscopy; CVFF, consistent valence force field; DMSO, dimethylsulphoxide; FT-IR, Fourier transform infrared spectroscopy; HOHAHA, homonuclear Hartmann–Hahn experiments; HPLC, high-performance liquid chromatography; MBHA, 4-methyl benzhydrylamine; NMR, nuclear magnetic resonance spectroscopy; NOE, nuclear Overhauser effect; NOESY, nuclear Overhauser enhancement spectroscopy; pro-OT/Np, precursor for ocytocin and neurophysin; ROESY, rotating frame nuclear Overhauser enhancement

Address for correspondence: Prof. Carlo Di Bello, Institute of Industrial Chemistry, 9, via Marzolo, 35131 Padova, Italy.

CCC 1075-2617/95/040251-15

spectroscopy; TFE, 2,2,2-trifluoroethanol; TMS, tetramethylsylane; TPPI, time proportional phase incrementation.

INTRODUCTION

Post-translational proteolytic processing of inactive precursors represents a key event in the maturation of many bioactive peptides. This rather specific cleavage takes place mainly at sites formed by single or paired basic residues [1]; the basic amino acids are then removed from the resulting fragments by exopeptidases, and peptides terminating with a Gly residue undergo C-terminal amidation [2].

To date, little is known about processing enzymes and their mechanism of action. So, only a few endoproteases, which have been isolated and completely purified, are considered as candidate processing enzymes [2–10]. Moreover, some cDNAs encoding subtilisin-like protease sequences have been identified as inducers of various pro-proteins in *in vivo* processing [11–13].

The precursor for ocytocin and neurophysin (pro-OT/Np) is a relatively simple prohormone in which ocytocin occupies the N-terminal segment of the molecule, whereas neurophysin is C-terminal. The Gly-Lys-Arg processing sequence connects the two domains and constitutes the site where endoproteolytic cleavage occurs both *in vivo* and *in vitro* [14–16].

Previous studies using a series of peptides reproducing, or mimicking, the various segments of the pro-ocytocin processing domain, and a putative, dibasic selective, convertase isolated from bovine tissues, demonstrated the importance of certain residues in substrate recognition and processing by this protease [16, 17]. Moreover, site-directed mutagenesis performed on human pro-somatostatin suggested a possible key role of proline residues in favouring the adequate conformation for *in vivo* processing in transfected mammalian cells [18].

Preliminary work suggesting that prohormone processing could take place at paired basic residues preferentially when these residues form part of ordered structures, e.g. with a β-turn on one side and a helix on the other, has been already published [19–21].

This paper reports a detailed CD, FT-IR and ^{1}H-NMR study on several model peptides corresponding to the primary processing region of pro-ocytocin. These new experimental results include acid–base CD titrations, FT-IR spectra under conditions corresponding to those utilized in the NMR experiments, and the effect of isotopic exchange. A theoretical model elaborated from energy minimization calculations is also presented.

MATERIALS AND METHODS

Synthesis

Peptides (Table 1) were synthesized by standard solid-phase methods [22] on an Applied Biosystems 431A apparatus using Boc chemistry and a MBHA resin for all C-terminal amidated peptides; a chloromethyl-polystyrene–1% divinylbenzene resin functionalized with Boc-Leu-OH was used for the synthesis of peptide XXIV-OH. Both resins were purchased from Novabiochem (Läufelfingen, Switzerland). Peptide purification and analyses were performed by HPLC using an ACN/H_2O mixture containing 0.05% TFA
as eluent. A Waters C_{18} Delta-Pak (100 Å, 3.9 × 150 mm) column was used for analytical purposes and a Waters C_{18} Delta-Pak (100 Å, 7.8 × 300 mm) column for semipreparative runs. Amino acid composition analysis, after acid hydrolysis, amino-terminal sequencing and fast atomic bombardment mass spectrometry gave the expected results. The four pro-ocytocin/neurophysin related peptides used in the present study are numbered as in [17]. All peptides are in the C-terminal amide form unless otherwise stated.

CD Measurements

CD spectra were performed at room temperature (~25 °C) using a Jasco model J-500 automatic recording circular dichrograph equipped with a Jasco 500 N data processor. Cylindrical fused quartz cells of 0.1 cm pathlength were employed. The CD instrument was standardized with D-10 camphorsulphonic acid and epiandrosterone. Spectra are reported in units of mean residue ellipticity (peptide molecular weight/number of amino acids) $[\theta]_R$ (deg × cm^2 × dmol^{-1}). Peptide samples were prepared by dissolving known quantities in a minimum

Table 1

Peptide	Sequences
XXIV	Leu^8-Gly-Gly-Lys-Arg-Ala-Val-Leu^{15}
XXV	Pro^7-Leu^8-Gly-Gly-Lys-Arg-Ala-Val-Leu^{15}
XXIII	Leu^8-Gly-Gly-Lys-Arg-Aia-Val-Leu-Asp^{16}-Leu-Asp-Val-Arg^{20}
[Pro^7]-XXIII	Pro^7-Leu^8-Gly-Gly-Lys-Arg-Ala-Val-Leu-Asp^{16}-Leu-Asp-Val-Arg^{20}

amount of water to which TFE was added up to a final content of 95% (v/v). Peptide concentrations were determined by mass and by peptide content using peptide-hydrolysate amino acid analysis (Waters Pico Tag Systems). They ranged from 4.5×10^{-5} to 1.0×10^{-2} M.

FT-IR Measurements

FT-IR spectra were recorded at room temperature using a Jasco 300-E FT-IR instrument. Cells with a CaF_2 window and a 0.1 mm (for D_2O solutions) or 0.2 mm (for TFA, TFE/DMSO and DMSO solutions) pathlength were employed throughout. To obtain spectra with a satisfactory signal to noise ratio, up to 100 scans were collected for each experiment. Solvent baseline spectra were recorded under identical conditions. Data were managed (including apodization, solvent subtraction and derivatization) using a personal computer with Jasco FT version 1.00.03 for Windows version 3.1 Spectra calc. software. Owing to the low solubility of the two larger peptides in TFE, samples for experiments with XXIII and [Pro^7]-XXIII in TFE/DMSO were prepared by dissolving known peptide quantities in a minimum amount of DMSO and then adding TFE up to a final content of 80% (v/v). N-Deuterated samples were prepared by dissolving weighed amounts (1–1.5 mg) of peptide in D_2O (200 µl), and by keeping the solution for 2 h at room temperature in order to obtain complete H–D exchange. Finally, the H–D exchanged samples were lyophilized and solubilized in DMSO (100 µl). Peptide concentrations in all the experiments ranged from 5.7×10^{-3} to 1.5×10^{-2} M.

NMR Measurements

NMR studies were carried out on a Varian Unity 400 and on a Bruker AM 400 spectrometer. Solutions were prepared by dissolving 4–6 mg of each peptide in 0.7 ml of the following solvents: DMSO-d_6 (99.99% isotopic purity, Aldrich); DMSO-d_6/H_2O, 70/30 (v/v) and 90/10 (v/v); TFE-d_3/H_2O, 70/30 (v/v) and H_2O/D_2O, 90/10 (v/v). All peptides exhibit in H_2O a pH of 4.0–4.5. The isotopic purities of D_2O and TFE-d_3 (Aldrich) were 99.9% and 99%, respectively. NMR chemical shifts were referred to internal tetramethylsylane (TMS) in the case of DMSO and TFE solutions, and to internal 3-(trimethylsilyl)-propionic acid-2,2′,3,3′-d_4 in the case of water solutions.

Proton chemical shift assignments were made with the aid of 2D-techniques, such as COSY [23], HOHAHA [24], NOESY [25] and ROESY [26]. 2D-spectra were always run in phase-sensitive mode using the TPPI or the States–Haberkorn method. All 2D-spectra were acquired at 298 K. This time-domain matrix was formed of 512×2048 complex data points for NOESY and ROESY spectra, and of 512×4096 complex data points for COSY and HOHAHA experiments. All experiments were zero filled in F1 before transformation. Gaussian, sine-bell and square function were used for resolution enhancement in both dimensions. HOHAHA experiments with a time of 70 ms were shown to provide optimal magnetization transfer. ROESY and NOESY experiments were performed with mixing times in the range of 100–400 ms. Temperature coefficients were measured over the 298–318 K temperature range.

Computational Details

Starting models for energy minimization were derived from NOE data. Energy minimizations were performed with a Silicon Graphics workstation IRIS 4D25GT Turbo computer, using the DISCOVER program of the Discover package of Biosym Technologies with the '*ab initio* potentials' of the CVFF [27–29]. Every energy minimization was performed including NOE effects as interatomic constraints and using the conjugate gradient method [30]. Several minimization runs were performed until the maximum derivate was less than 0.01 Kcal mol^{-1} [31, 32]. No attempts to introduce the effects of solvation were made so far owing to the complexity of such calculations.

RESULTS AND DISCUSSION

CD Measurements

Figure 1 (A) and (B) reports the CD spectra of peptides XXIV and XXV, respectively, in TFE/H_2O (95/5) with increasing quantities of NaOH and in the presence of excess HCl. In TFE/H_2O ($R = 0$), CD patterns were characterized by two negative maxima around 200 and at 218–224 nm, indicating the existence of a conformational equilibrium between aperiodic structures and folded conformations [21]. Measurements carried out at various peptide concentrations (10^{-2}–10^{-4} M) do not show significant effects on the spectral patterns of either peptide. Progressive addition of NaOH caused an enhancement of the spectral intensity, a red shift of the band situated at 199–200 nm, and the appearance or the increase of a positive maximum below 200 nm. These observations indicate that neutralization of the basic

groups induces a shift in the conformational equilibrium towards populations with folded conformations. The presence of excess HCl, instead, produced only a slight modification in the CD spectra of XXIV and XXV, compared to patterns obtained at $R = 0$.

Figure 2 (A)–(D) shows the CD titration curves of peptides XXIII and [Pro^7]-XXIII in TFE/H_2O. The spectra of these peptides were characterized, with respect to peptides XXIV and XXV, by a more pronounced red shift of the two negative maxima, the presence of a positive maximum below 200 nm, and a more significant enhancement in the intensity of the two negative bands, suggesting a greater contribution of folded conformations to the dichroism in the two larger fragments. As observed for XXIV and XXV, addition of NaOH indicated that a progressive neutralization of the basic residues and an ionization of the acidic ones cause an enhancement in the population of conformers in ordered secondary structures. Unlike XXIV and XXV, neutralization of the acidic groups produced a considerable enhancement in the dichroic signal and a red shift of the two negative maxima, as demonstrated by the titration curves with HCl. The latter observation suggests that neutralization of the acidic groups also induces an enhancement in the population of conformers in ordered secondary structure. Hence, the CD spectral pattern in the presence of acid resembles that typical of partially helical peptides [33].

In order to compare the results obtained by CD with those obtained by FT-IR techniques (see below), the CD spectra of peptides XXIII and [Pro^7]-XXIII in TFE/H_2O have been recorded at various peptide concentrations (10^{-2}–10^{-5}). Interestingly, the spectra recorded at a high peptide concentration show a significant increase of the signal intensity accompanied by a red shift of the negative bands. This behaviour is similar to that observed in the presence of excess HCl and could be attributed to the possibility of amphiphilic interactions in the C-terminal segment of the molecule.

FT-IR Measurements

The FT-IR spectra of peptides XXIV, XXV, XXIII and [Pro^7]-XXIII in TFE or TFE/DMSO (80/20), D_2O and DMSO are reported in Figures 3 and 4. In the amide I region, the second derivative patterns exhibit similar trends for the different peptides. In particular, the spectra in D_2O are dominated by an intense band with a maximum located between 1650 and 1640 cm^{-1}, a region which is usually assigned to unordered structures [34–36]; only minor absorptions are detectable in the β-turns 1690–1666 cm^{-1} region [34–36]. In DMSO, the computed second derivative patterns show intense bands centred around 1665 cm^{-1} accompanied by more pronounced bands around 1690 cm^{-1}. A similar trend was observed in TFE or TFE/DMSO, where the major band is shifted around 1660 cm^{-1}, while the minor band observed in DMSO is centred around 1680 cm^{-1}. The weak 1720–1710 cm^{-1} band in the longer

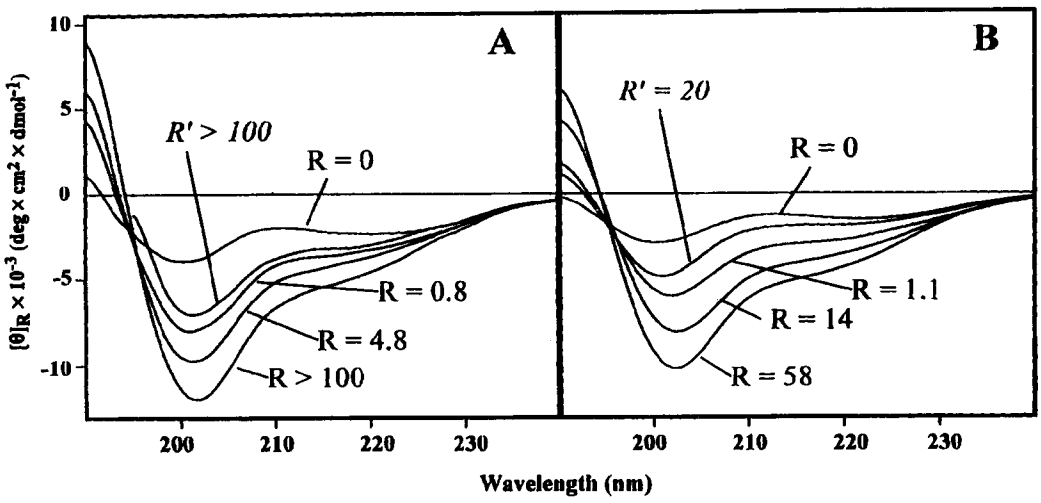

Figure 1 CD spectra of peptide XXIV (A) and XXV (B) in TFE/H_2O (95/5 v/v) with increasing amounts of NaOH (R), and in the presence of an excess of HCl (R'). R and R' represent the molar ratio of NaOH and HCl with respect to the number of equivalents of ionizable groups present in the sample.

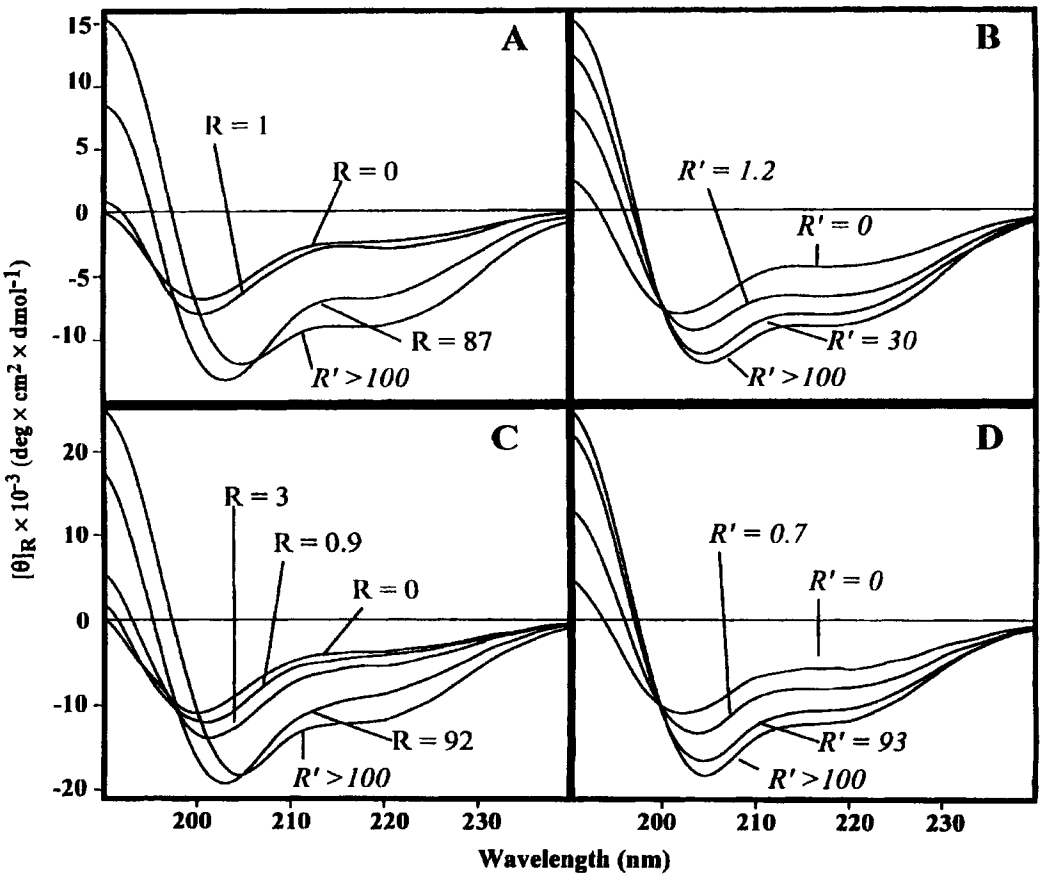

Figure 2 CD spectra of peptide XXIII (A and B) and [Pro^7]-XXIII (C and D) in TFE/H_2O mixture (95/5 v/v) with increasing amounts of NaOH (*R*) or HCl (*R'*). *R* and *R'* represent the molar ratio of NaOH and HCl with respect to the number of equivalents of ionizable groups present in the sample.

peptides can be assigned to the β-carboxyl groups of Asp^{16} and Asp^{18}; the assignment of the weak band centred at 1630–1610 cm^{-1} is more problematic. This latter band is located in the region of β-sheet absorption; however, CD measurements at different peptide concentrations seem to exclude the presence of a significant population of intermolecular β-aggregates. It should also be noted that, according to recent studies, β-turns are likely to give contributions in the region below 1640 cm^{-1} [37]. In spite of the margins of uncertainty connected to this technique [34–36, 38], the above features may be attributed to the existence of an equilibrium between populations of random and folded peptide molecules with an increase of structure from D_2O to organic solvents.

This hypothesis is substantiated by experiments performed in DMSO on peptides in which the amide protons were exchanged by deuterium. With respect to the results obtained with peptide with no isotopic exchange, the absorption attributed to β-turn structures around 1690–1688 cm^{-1} is shifted to lower wavenumbers in the spectra of deuterated samples, while the major component of the amide I band is only sparingly affected by H–D exchange. Since the amide I band arises primarily from the stretching mode of the carbonyl moiety, with only a minor contribution from the N–H vibration, H–D exchange has only little effect on the frequency of this band. Therefore, the significant shift observed in the high wavenumber component of amide I band could be attributed to the effect of H–D exchange on the absorption of intramolecularly hydrogen-bonded carbonyl groups [39], and, possibly, to a peptide group involved in a β-turn structure. The difference in the absorption observed between deuterated and not deuterated samples cannot be explained as an effect of exchange on sidechains of Arg and Lys residues, which in H_2O give IR bands respectively at 1673 and 1633 cm^{-1}, and 1629 and 1526 cm^{-1} [40] and, in D_2O are shifted to 1608 and 1586 cm^{-1}, in the case of Arg [41]. Moreover, measurements performed on Arg did not show any significant effect

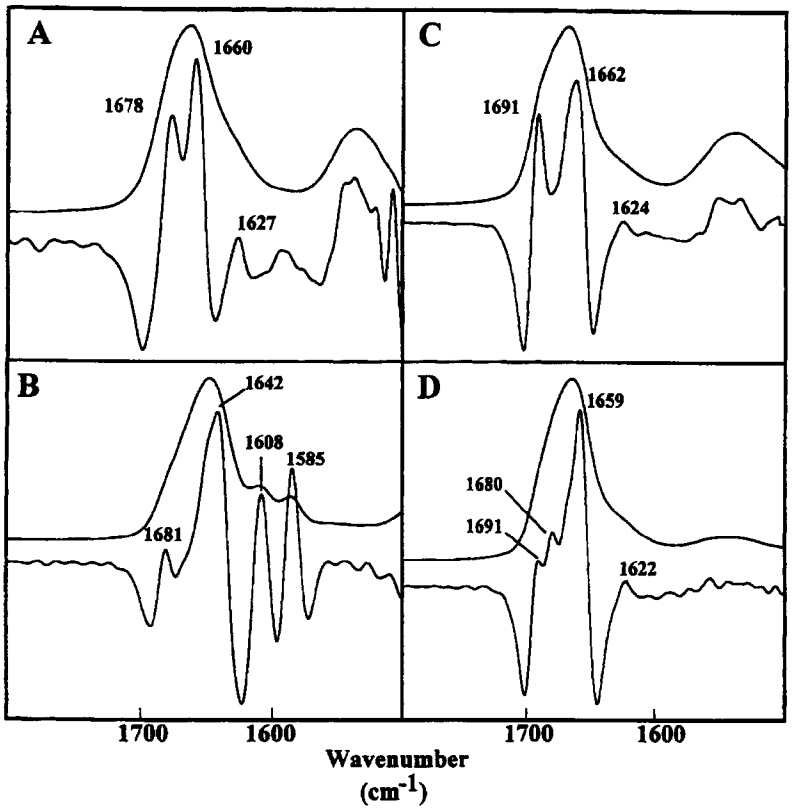

Figure 3 FT-IR of peptide XXIV in the amide I region in TFE (A), D_2O (B) and DMSO (C). (D) refers to the H–D exchanged sample in DMSO solution. In each panel the upper line represents the original spectrum, while the lower line refers to the opposite of the corresponding second derivative.

of DMSO on the position of the guanidinium group IR bands.

NMR Measurements

Peptide XXIV. NMR spectra in DMSO, DMSO/H_2O, TFE/H_2O and H_2O were analysed. Backbone coupling constants, amide proton temperature coefficients and conformationally informative NOE effects, measured in DMSO/H_2O, are reported in Table 2.

In DMSO/H_2O, weak NH–NH interactions appear in the NOESY 2D spectrum (Figure 5A) and involve the two peptide segments, including Gly^9, Gly^{10} and Lys^{11} on one side and Ala^{13}, Val^{14} an Leu^{15} on the other (Table 2). Assuming that these weak NOE effects could be attributed to weakly populated ordered structures, the experimental data fit two β-turns in the Leu^8-Lys^{11} and Arg^{12}-Leu^{15} segments [42]. The relatively lower values of the $J_{\alpha N}$ coupling constants in this solvent mixture support this assumption.

In the other solvents, NMR parameters point to disordered conformers; in fact, backbone coupling constants are similar to those found for random structures. In addition, relatively high temperature coefficients of amide protons, together with the observation of no NOE effects other than sequential ones between backbone α-CH_i and $NH_{(i+1)}$ support this conclusion.

Peptide XXV. NMR parameters were measured in the same solvents as described above and are reported in Table 3. Proton resonance assignments were carried out mostly by 2D techniques. Unlike the previous case, NH–NH NOE interactions that are relevant to secondary structure implications [42], can be determined not only in DMSO/H_2O but also in pure DMSO. Measurements at two different temperatures show the same weak intramolecular NOE effects between Gly^9 and Gly^{10}, and between Ala^{13} and Val^{14} (Figure 5(B)). Assuming that these effects refer to weakly populated ordered species, the data are consistent with the existence of two β-turns in the

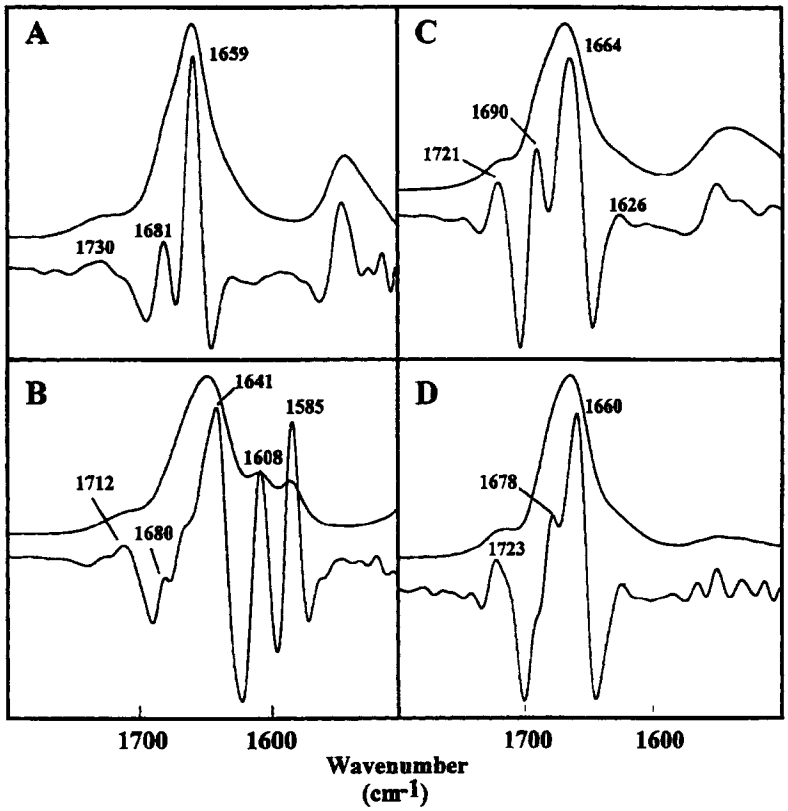

Figure 4 FT-IR of peptide XXIII in the amide I region in TFE/DMSO (A) mixture, D_2O (B) and DMSO (C). (D) refers to the H–D exchanged sample in DMSO solution. In each panel the upper line represents the original spectrum, while the lower line refers to the opposite of the corresponding second derivative.

peptide fragments Pro^7-Gly^{10} and Lys^{11}-Val^{14}. By simple comparison of these NOE effects with those seen for peptide XXIV, it appears very likely that the two β-turns are architecturally distinct. Molecular mechanic calculations on both peptides (see below) give low-energy solutions compatible with this hypothesis.

Peptide XXIII. NMR parameters were measured in DMSO and DMSO/H_2O; proton chemical shifts in both solvents were similar to those of the two shorter fragments. Table 4 shows backbone coupling constants, amide proton temperature coefficients and conformationally informative NOE effects measured in the cryoprotective mixture DMSO/H_2O (70:30).

Table 2 *Peptide XXIV*: Leu^8-Gly^9-Gly^{10}-Lys^{11}-Arg^{12}-Ala^{13}-Val^{14}-Leu^{15}

AA	d_{NN}[a]	$d_{\alpha N}$[b]	$^3J_{NH\alpha}$ (Hz) XXIV-NH_2	$^3J_{NH\alpha}$ (Hz) XXIV-OH	$\Delta\delta/\Delta T$ (ppb/K) XXIV-NH_2	$\Delta\delta/\Delta T$ (ppb/K) XXIV-OH
Leu^8			–			
Gly^9			5.7	5.5	−4.9	−5.1
Gly^{10}	Gly^9		5.8	5.6	−4.4	−4.9
Lys^{11}	Gly^{10}	Gly^{10}	7.0	7.3	−4.2	−4.2
Arg^{12}			7.0	7.6	−5.0	–
Ala^{13}		Arg^{12}	6.6	7.1	−5.2	−5.1
Val^{14}	Ala^{13}	Ala^{13}	8.1	8.4	−4.9	−4.6
Leu^{15}	Val^{14}	Val^{14}	7.9	6.2	−4.8	–

[a] d_{NN}: NOE contacts between NH_{i+1} and NH_i.
[b] $d_{\alpha N}$: NOE contacts between NH_{i+1} and αCH_i.

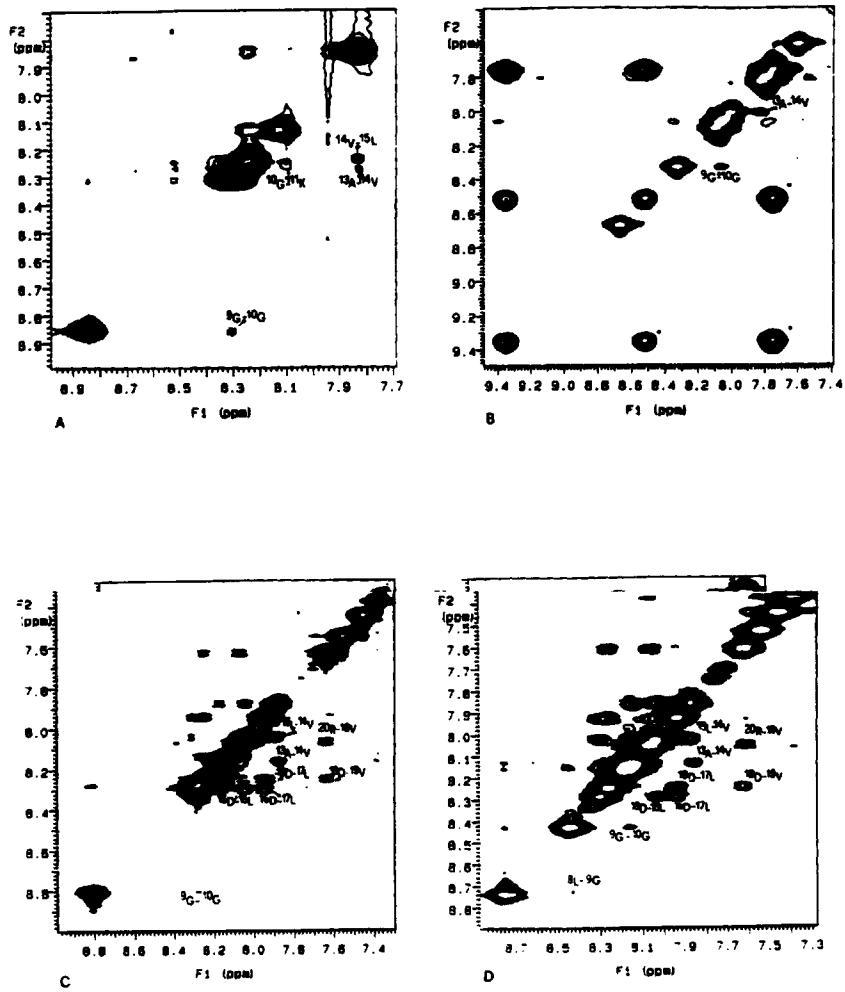

Figure 5 2D-NOESY spectra NH–NH regions acquired at 298 K in DMSO/H_2O for peptides: (A) XXIV; (B) XXV; (C) XXIII; (D) [Pro^7]-XXIII.

The NOE effects (Figure 5(C)) in this case are considerably stronger compared with those observed for peptides XXIV and XXV, and thus enable a possible β-turn structure in the Leu^8-Lys^{11} segment, and a helical structure in the C-terminal Ala^{13}-Arg^{20} fragment to be postulated with a higher degree of confidence.

It should also be pointed out that backbone coupling constants for peptide XXIII reveal a trend towards lower values in going from DMSO to DMSO/H_2O, in agreement with the NOE data indicating that a higher population of a folded structure exists in the latter solvent.

Peptide (Pro^7)-XXIII. NMR parameters were measured in DMSO and DMSO/H_2O. Backbone coupling con stants, amide proton temperature coefficients and NOE effects are reported in Table 5. NH–NH NOE effects were observed both in DMSO and DMSO/H_2O (Figure 5(D)) and were stronger than those observed for peptides XXIV and XXV. In particular, the NOEs between consecutive peptide NHs along the C-terminal segment, starting from Ala^{13} to the last Arg^{20} residue, support the possibility of a helical-type structure in the C-terminal sequence.

More structurally informative NOE effects, involving the residues Gly^9-GLy^{10}, were found in the DMSO/H_2O system (Table 5). Based on NOEs, it is possible to postulate a folded region in the N-terminal part of this peptide, and this is compatible with a β-turn involving the Pro^7-Gly^{10} segment.

Molecular Models

Even though computational data on flexible molecules must be taken with some caution, particularly in the absence of solvation, energy minimizations

Table 3 *Peptide XXV*: Pro^{7}-Leu^{8}-Gly^{9}-Gly^{10}-Lys^{11}-Arg^{12}-Ala^{13}-Val^{14}-Leu^{15}

AA	d_{NN}[a]	$d_{\alpha N}$[b]	$^{3}J_{NH\alpha}$ (Hz)	$\Delta\delta/\Delta T$
Pro^{7}			–	
Leu^{8}		Pro^{7}	8.0	−3.3
Gly^{9}		Leu^{8}	5.7	−5.2
Gly^{10}	Gly^{9}		5.8	−4.1
Lys^{11}			7.6	−4.0
Arg^{12}			7.9	−4.6
Ala^{13}			7.2	−4.2
Val^{14}	Ala^{13}	Ala^{13}	9.1	−4.5
Leu^{15}			8.1	−4.0

[a] d_{NN}: NOE contacts between NH_{i+1} and NH_i.
[b] $d_{\alpha N}$: NOE contacts between NH_{i+1} and αCH_i.

Table 4 *Peptide XXIII*: Leu^{8}-Gly^{9}-Gly^{10}-Lys^{11}-Arg^{12}-Ala^{13}-Val^{14}-Leu^{15}-Asp^{16}-Leu^{17}-Asp^{18}-Val^{19}-Arg^{20}

AA	d_{NN}[a]	$d_{\alpha N}$[b]	$^{3}J_{NH\alpha}$ (Hz)	$\Delta\delta/\Delta T$
Leu^{8}			–	–
Gly^{9}		Leu^{8}	5.6	−5.5
Gly^{10}	Gly^{9}	Gly^{9}	5.2	−5.2
Lys^{11}	Gly^{10}	Gly^{10}	6.7	−4.8
Arg^{12}			7.7	−5.7
Ala^{13}			7.0	−5.4
Val^{14}	Ala^{13}		7.3	−5.1
Leu^{15}	Val^{14}	Val^{14}	6.1	−5.5
Asp^{16}	Leu^{15}		6.7	−6.5
Leu^{17}	Asp^{16}	Asp^{16}	7.3	−5.2
Asp^{18}	Leu^{17}		8.3	−4.4
Val^{19}	Asp^{18}	Asp^{18}	7.7	−4.0
Arg^{20}	Val^{19}	Val^{19}	8.3	−4.9

[a] d_{NN}: NOE contacts between NH_{i+1} and NH_i.
[b] $d_{\alpha N}$: NOE contacts between NH_{i+1} and αCH_i.

were performed in order to build plausible molecular models based on the experimental NOE data. The NH–NH interactions suggest a possible structure for peptide XXIV that involves two type I β-turns, the first starting from Leu^{8}, and the latter from Arg^{12}; both imply the formation of intramolecular H-bonds between Lys^{11} NH and Leu^{8} CO, and between Leu^{15} NH and Arg^{12} CO. Application of minimization methods shows that this conformational model is stable, and represents an energy minimum for the structure. Moreover, an analysis of the H-bond pattern discloses the presence of additional hydrogen bonds between Leu^{8} NH and Lys^{11} CO, and between Leu^{8} NH and ε-N of the Arg^{12} sidechain, thus suggesting the existence of successive hydrophobic and hydrophilic domains with Lys and Arg sidechains pointing toward opposite regions (Figure 6(A)).

In the case of peptide XXV, in which a Pro residue

Table 5 *Peptide [Pro^{7}]-XXIII*: Pro^{7}-Leu^{8}-Gly^{9}-Gly^{10}-Lys^{11}-Arg^{12}-Ala^{13}-Val^{14}-Leu^{15}-Asp^{16}-Leu^{17}-Asp^{18}-Val^{19}-Arg^{20}

AA	d_{NN}[a]	$d_{\alpha N}$[b]	$^{3}J_{NH\alpha}$ (Hz)	$\Delta\delta/\Delta T$
Pro^{7}			–	–
Leu^{8}			7.2	−3.5
Gly^{9}	Leu^{8}		5.5	−5.6
Gly^{10}	Gly^{9}	Gly^{9}	5.9	−5.2
Lys^{11}			8.3	−4.2
Arg^{12}			8.3	−5.8
Ala^{13}			7.2	−4.4
Val^{14}	Ala^{13}		8.8	−4.8
Leu^{15}	Val^{14}	Val^{14}	8.3	−4.3
Asp^{16}	Leu^{15}		8.3	−5.9
Leu^{17}	Asp^{16}	Asp^{16}	8.3	−4.1
Asp^{18}	Leu^{17}		8.3	−5.9
Val^{19}	Asp^{18}	Asp^{18}	8.2	−3.1
Arg^{20}	Val^{19}	Val^{19}	7.7	−4.3

[a] d_{NN}: NOE contacts between NH_{i+1} and NH_i.
[b] $d_{\alpha N}$: NOE contacts between NH_{i+1} and αCH_i.

was added to the N-terminal part of peptide XXIV, two type II β-turns, starting from Pro^{7} and Lys^{11} respectively, were suggested by the NOE data. Four different models were built with all possible combinations of type I and type II β-turns in peptide segments 7–11 and 11–15. Each model was then tested with the minimization procedure, and the results indicated that the most stable structure is the one suggested by the NOE data. Analysis of the H-bond pattern shows an H-bond between Pro^{7} CO and Gly^{10} NH, an H-bond between Lys^{11} CO and Val^{14} NH, and an extra H-bond between Pro^{7} NH and Gly^{10} CO. According to these data, the structures of peptides XXV and XXIV would differ substantially. In fact (Figure 6(B)) the Lys and Arg sidechains in peptide XXV are on the same side of the molecule and determine two well-defined hydrophobic and hydrophilic domains. In addition, the most stable structure of peptide XXV is less stable than the corresponding peptide XXIV structure. This hypothesis provides a possible explanation for the different NMR behaviour of the two compounds.

In the case of peptides XXIII and [Pro^{7}]-XXIII, two slightly different situations can be postulated (Figure 6(C) and (D)). In fact, both peptides share a β-turn structure in the N-terminal segment, namely a type I β-turn between Leu^{8} CO and Lys^{11} NH for peptide XXIII, and a type II β-turn between Pro^{7} CO and Gly^{10} NH for [Pro^{7}]-XXIII. Moreover, they are characterized in the C-terminal part by a similar helical structure starting from the Ala^{13} residue. These features result

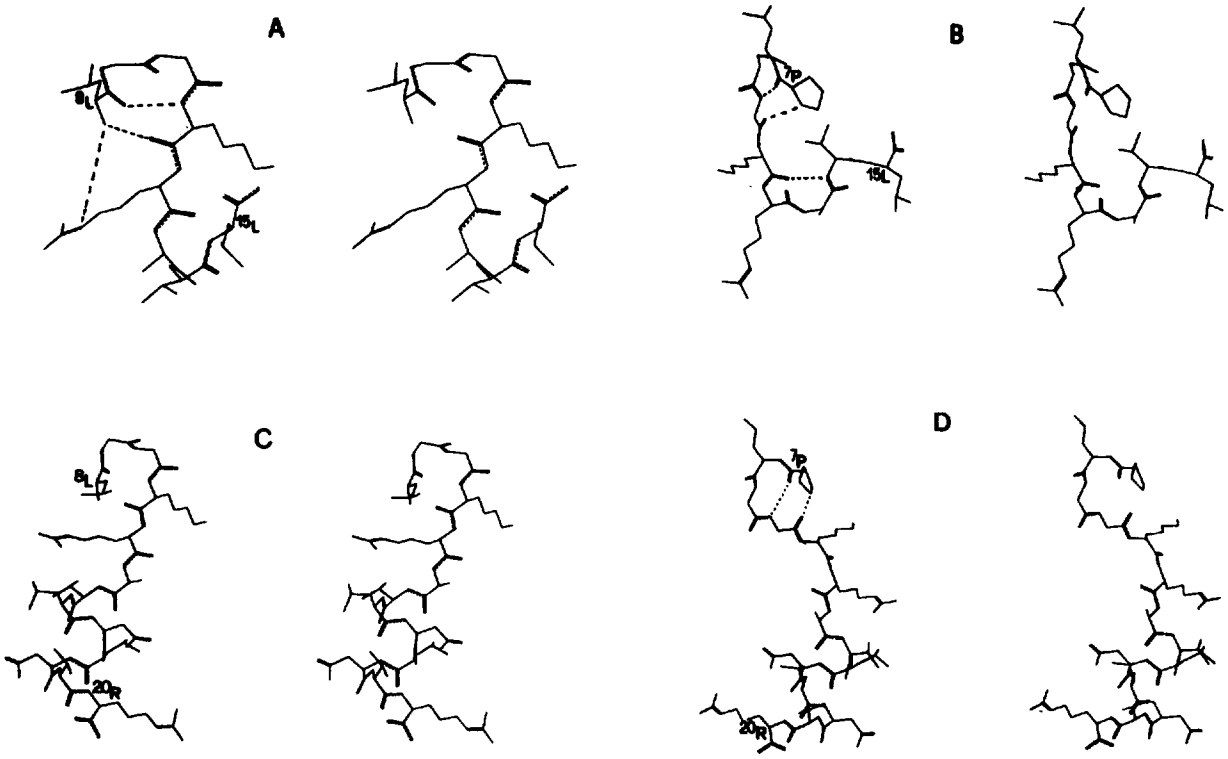

Figure 6 Stereoview of molecular models for peptides: (A) XXIV; (B) XXV; (C) XXIII; (D) [Pro^7]-XXIII.

in a different orientation for the Lys and Arg sidechains. In particular for peptides XXIII and XXIV, the sidechains are pointing toward opposite sides, while for peptides [Pro^7]-XXIII and XXV, the sidechains are on the same side of the molecule.

Effects of the C-terminal Group on Conformation

In view of the fundamental role played by the C-terminal carboxyamidated group in many bioactive peptides [43, 44] and considering the possible influence of C-terminal functionality on structure–function relationships, we carried out a comparative study on C-terminal amide peptide XXIV and the corresponding analogue with a C-terminal free carboxyl function.

The CD and FT-IR spectra of the two peptides were quite similar, despite the different C-terminal functional groups. In particular, the computed second derivative of the FT-IR spectra was characterized by bands located at the same wavenumbers, showing an identical contribution of ordered structure in both cases. However, it is worthwhile noting that NaOH titration of peptide XXIV-OH did not present the stabilization of ordered population shown by the amidated analogue.

The 1D-NMR spectra in the NH-amide region (between 8.0 and 8.4 p.p.m.) at 298 K of all peptides are reported in Figure 7. In particular Figure 7(II) shows that the NH resonances of the residues Gly^{10}, Arg^{12}, Ala^{13} and Leu^{15} are well resolved for the peptide in the amidated form, but are overlapping in the case of a free C-terminal carboxyl function. However, the temperature coefficients (Table 2) for the two compounds are very similar and show intermediate values, typical of averaged conformational structures; the same holds true for the $^3J_{NH\alpha}$. The observed NOE pattern is also the same for the two peptides, and therefore a molecular model can be assumed for both samples with the sidechains of Lys^{11} and Arg^{12} pointing toward opposite sides.

CONCLUSIONS

In order to provide information on the possible role of conformational preferences around the dibasic moiety representing the processing site of the pro-ocytocin/neurophysin system, several model peptides were examined by different spectroscopic techniques such as CD, FT-IR, NMR and by energy minimization procedures.

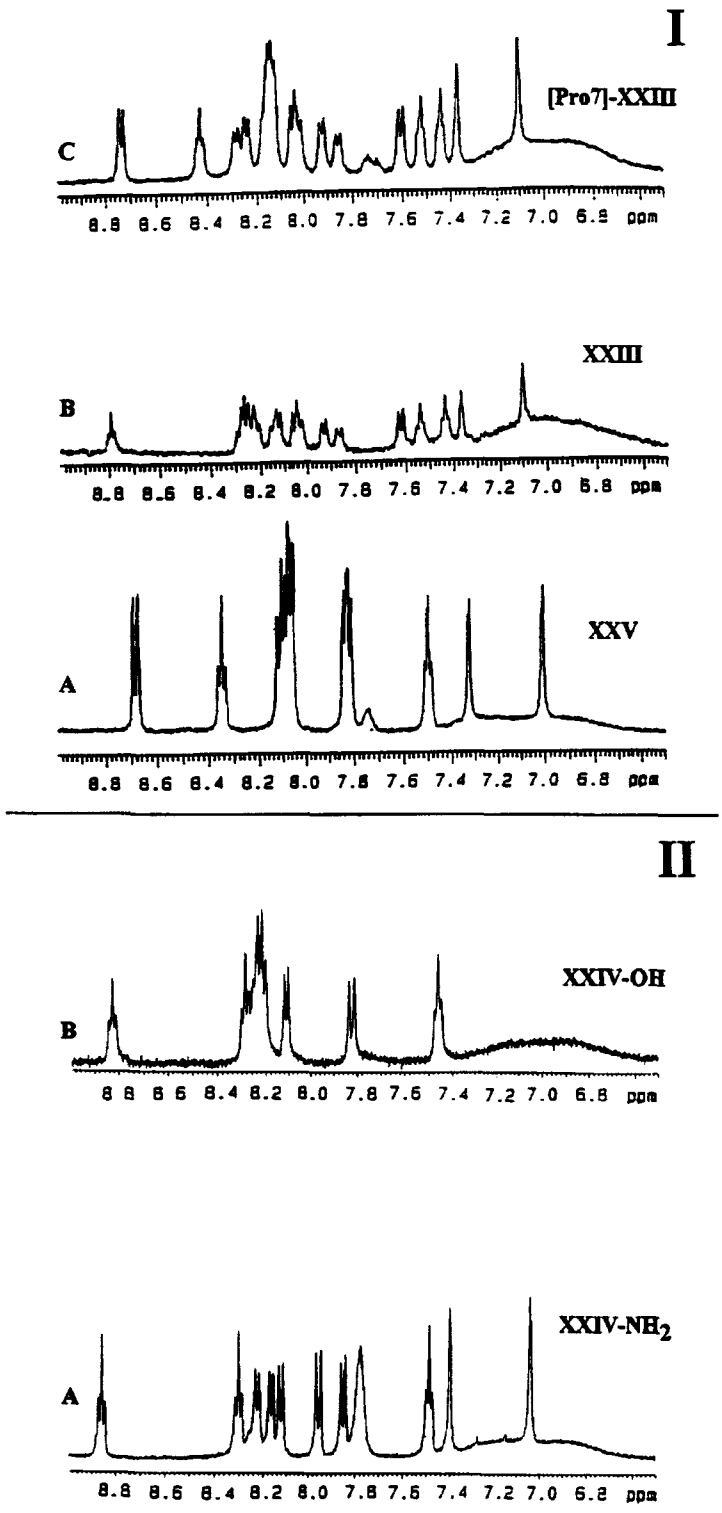

Figure 7 1D spectra of amide regions acquired at 298 K in DMSO/H_2O (70/30 v/v) for peptides: (I) (A) XXV, (B) XXIII, (C) [Pro^7]-XXIII and, (II) (A) XXIV-NH_2, (B) XXIV-OH.

CD measurements, in different solvents, suggest the existence of conformational equilibria between aperiodic and folded structures, thus confirming the prediction of a remarkable flexibility for all the peptides examined. Thus, they appear to be almost completely random in water and tend to assume more ordered conformations in TFE/H_2O (95/5), a solvent which is known to promote structuration [45]. Since in the case of peptides containing acidic and basic amino acids in their sequences the position of equilibrium between different conformers is influenced by the charge of the sidechains of the ionizable residues [46], acidic and basic titration experiments of peptide solutions in TFE/H_2O were performed. In the presence of NaOH, experimental data show that neutralization of the sidechains of Lys^{11} and Arg^{12} induces enhancement, and/or stabilization of molecular populations in ordered structures. In this respect, results obtained with the two larger peptides, XXIII and [Pro^7]-XXIII, are rather interesting; indeed, titration with NaOH showed a conformational behaviour similar to that observed with the two shorter fragments (XXIV and XXV), i.e. an enhancement of the populations in folded conformations. Moreover, unlike peptides XXIV and XXV, where no significant effects on the conformational equilibrium were observed by the addition of acid, in the case of XXIII and [Pro^7]-XXIII, acidic titration led to an enhancement of the populations in folded conformations. Interestingly, the pattern of the CD spectra indicates the contribution of a probable helical structure, located in the C-terminal segment of both peptides between Ala^{13} and Arg^{20}, that is stabilized by neutralization of the sidechains of Asp^{16} and Asp^{18}. This conformational transition of a helix-aperiodic structure is confirmed by the presence of an isodichroic point in the CD spectra obtained at various acid concentrations (Figure 2(B) and (D)). Such a transition most likely involves only the C-terminal region of XXIII and [Pro^7]-XXIII, where the two acidic residues are located.

The FT-IR spectra of peptides XXIII and [Pro^7]-XXIII in TFE/DMSO are similar to those previously obtained in TFE/D_2O 90/10 v/v [21] and this allows a good correlation between the CD and FT-IR data. In particular, the FT-IR spectra in the amide I region, within the limits of this technique, seem to confirm the results obtained by CD, i.e. the existence of a significant population with ordered secondary structure. Moreover, the analysis of the data supports the capability of such model peptides to assume ordered structures possibly containing β-turns. As a matter of fact, the spectra of the four fragments in DMSO indicate the contribution of two major components, the first located at 1665 cm^{-1}, assignable to carbonyls exposed to solvent [39, 47], and the second located at a higher wavenumber (1690 cm^{-1}), attributed instead to carbonyls involved in an intramolecular hydrogen bond. The 1690 cm^{-1} band does not seem to be compatible with the existence of a helical structure, that according to literature data [34–37] should present an absorption band around 1655 cm^{-1}. On the other hand, both theoretical [48] and solution studies [34–37] agree in assigning absorptions in the 1690–1665 cm^{-1} region to different β-turn types. Thus, it seems reasonable to assign to this component the contribution of ordered structures containing one or more β-turns. This hypothesis is confirmed by the results obtained after isotopic exchange; in fact, the H–D exchange causes a significant variation in the position of the band located at a higher wavelength, whereas the shift observed for the lower wavelength band is more limited. The amide I absorption presents two bands also in TFE and TFE/DMSO, which are located at lower wavelength compared with the ones observed in DMSO. The 1660 cm^{-1} band could be reasonably attributed to carbonyl groups exposed to solvent and this band was located in DMSO at 1665 cm^{-1}. Such a shift is compatible with the formation of hydrogen bonds between free carbonyl groups and TFE. Owing to the proximity between the IR absorptions of aperiodic and helical structures, contributions of putative helical segments, which would be particularly difficult to detect, cannot be excluded. The second band at 1678 cm^{-1} is attributed, as was the case in DMSO, to a carbonyl not involved in helix or in aperiodic disordered structures, but likely to be part of a β-turn. Taken together, the FT-IR data seem to indicate that, both in TFE and DMSO, the four model peptides examined present populations of molecules in ordered secondary structures that could be reasonably attributed to β-turns and, possibly, to helical segments.

More informative from a structural point of view are the results obtained by NMR; because of its different time scale, NMR averages out the contributions of random and folded conformations and consequently faint, or negligible, NOE effects could be detected in solvents such as H_2O and TFE/H_2O. Interestingly, when more viscous media such as DMSO and DMSO/H_2O were used, the presence of folded structures could be revealed [49]. This behaviour was particularly evident in the case of the two larger peptides, namely XXIII and [Pro^7]-XXIII, that exhibited significant NOE effects in DMSO/H_2O.

By combining the results obtained by the different spectroscopic techniques, particularly by NMR and FT-IR in DMSO, with computer modelling techniques, the following hypothesis for a possible structure of our model peptides could be drawn. In peptide XXIV, which is formed by eight amino acids spanning positions 8–15 of the natural prohormone, two type I β-turns appear to characterize a folded structure in which the two polar Arg and Lys sidechains lie on opposite sides (Figure 6(A)). The addition of a Pro residue (peptide XXV) in position 7 causes a structural modification. The two type I β-turns are converted into two type II β-turns, the first of which includes the Pro^7 residue at the *i* position. As a consequence, the Arg and Lys sidechains are now located on the same side of the molecule, thus forming a hydrophilic region (Figure 6(B)). In the larger peptides, namely XXIII and [Pro^7]-XXIII, which are extended at the C-terminus by five residues, spanning the 16–20 sequence of the native prohormone, the N-terminal β-turn exhibits the same differences previously found for the shorter peptides, i.e. a type I β-turn for XXIII and a type II β-turn for [Pro^7]-XXIII. As a consequence, the Arg and Lys sidechains would be once again oriented in opposite sides. The second β-turn, instead, may become, in both peptides, the initiator of a helical stretch involving the Ala^{13}-Arg^{20} peptide segment.

In conclusion, the experimental data collected by different spectroscopic techniques and by computational methods seem to be compatible with the hypothesis of a possible role of ordered secondary structures in pro-ocytocin processing. Such structures are very likely characterized by two β-turns of different type in the shorter peptides (XXIV and XXV) and by one β-turn of different type in the N-terminal region and a common α-helical segment involving the C-terminal sequence in the two larger peptides (XXIII and [Pro^7]-XXIII). Our present findings do not allow, however, a straightforward correlation between the β-turn subtype and/or the relative orientation of the Lys/Arg sidechains and substrate processing, as was confirmed by the results of *in vitro* experiments conducted with a putative prohormone convertase [21]. Activity data indicated the same kinetic parameters for both peptide XXIII, in which the sidechains of Lys^{11} and Arg^{12} are positioned on the same side, and [Pro^7]-XXIII, in which these sidechains are oriented in opposite ways. In addition, both peptide XXIII with a type I β-turn, and peptide [Pro^7]-XXIII with a type II β-turn were found to be active. Moreover, elongation of the peptide chain from the C-terminal side by five residues in the inactive peptide XXIV (which originates peptide XXIII) brings about a backbone conformational modification involving the second β-turn, which now becomes the initial part of a helical stretch and, interestingly, restores biological activity.

Ongoing studies on different models, including the 1–20 sequence, may give further insights and ultimately, provide a definitive demonstration that the particular prohormone domain surrounding the dibasic doublet, which is mostly disordered in aqueous solution, can assume a privileged secondary structure organization in the entire 1–20 peptide which includes the ocytocin ring and/or upon binding to the active site of maturation enzymes, thus imparting the recognition signal for the processing machinery.

Finally, it is worth noting that proteolytic processing has been shown to initiate in several secretory systems in the *trans*-most Golgi network [50–52] and within the nascent secretory granules, i.e. in highly hydrophobic membrane surroundings. Therefore, although most of the peptides studied exhibited disordered conformations in water, it can be envisioned that both the endoprotease binding site and the membrane environment provide most of the energy necessary to shift conformational equilibria toward the ordered peptide conformers.

Acknowledgements

This work was supported by funds from the Italian CNR (Progetto Chimica Fine II) and Italian MURST 40 and 60% and by the Ministère de l'Education Nationale et de la Récherche and the CNRS (URA 1682). NMR measurements were carried out on a Varian Unity 400, located at the Centro di Ricerca su Peptidi Bioattivi, and on a Bruker AM 400 spectrometer, located at the Centro Interdipartimentale di Metodologie Chimico-Fisiche of the Federico II University of Naples.

REFERENCES

1. T. J. Stoller and D. Shields (1989). The role of paired basic amino acids in mediating proteolytic cleavage of prosomatostatine. *J. Biol. Chem. 261*, 6922–6928.
2. N. J. Darby and D. G. Smyth (1990). Endopeptidases and prohormone processing. *Biosci. Rep. 10*, 1–13.
3. K. Mizuno and H. Matsuo (1984). A novel protease from yeast with specificity towards paired basic residues. *Nature 309*, 558–560.
4. P. Gluschankof, S. Gomez, A. Morel and P. Cohen (1987). Enzymes that process somatostatin precursors. A novel endoprotease that cleaves before the arginine-

lysine doublets is involved in somatostatine-28 convertase activity of rat brain cortex. *J. Biol. Chem. 262*, 9615–9620.

5. S. Gomez, P. Gluschankof, A. Lepage and P. Cohen (1988). Relationship between endo and exopeptidases in a processing enzyme system: activation of an endoprotease by the aminopeptidase B-like activity in somatostatine-28 convertase. *Proc. Natl. Acad. Sci. USA 85*, 5468–5472.
6. G. E. Maret and J. L. Fauchère (1988). Purification of an endoprotease from bovine adrenal medulla granules which cleaves in vitro at paired but not at single basic residues. *Anal. Biochem, 172*, 248–258.
7. R. S. Fuller, A. Brake and J. Thorner (1989). Yeast prohormone processing enzyme (KEX2 gene product) is a Ca^{2+}-dependent serine protease. *Proc. Natl. Acad. Sci. USA 86*, 1434–1438.
8. P. Kuks, C. Créminon, A. M. Leseney, J. Bourdais, A. Morel and P. Cohen (1989). Xenopus laevis skin Arg-Xaa-Val-Arg-Gly endoprotease. A highly specific protease cleaving after a single arginine of a consensus sequence of peptide hormone precursors. *J. Biol. Chem. 264*, 14609–14612.
9. I. Plevrakis, C. Clamagirand, C. Créminon, N. Brakch, M. Rholam and P. Cohen (1989). Proocytocin/Neurophysin convertase from bovine neurohypophysis and corpus luteum granules: complete purification, structure–function relationships, and competitive inhibitor. *Biochemistry 28*, 2705–2710.
10. J. Bourdais, A. Pierotti, H. Boussetta, N. Barre, G. Devilliers and P. Cohen (1991). Isolation and functional properties of an arginine-selective endoprotease from rat intestinal mucosa. *J. Biol. Chem 266*, 23386–23391.
11. G. Thomas, B. Thorne, L. Thomas, R. G. Allen., D. Hruby, R. Fuller and J. Thorner (1988). Yeast KEX2 endopeptidase correctly cleaves a neuroendocrine prohormone in mammalian cells. *Science 241*, 226–230.
12. R. Wise, P. Barr, M. Kiefer, A. Brake and R. Kaufman (1990). Expression of a human proprotein processing enzyme: correct cleavage at the von Willebrand factor precursor at a paired basic amino acid site. *Proc. Natl. Acad. Sci. USA 87*, 9378–9382.
13. L. Zollinger, C. Racine, P. Crine, G. Boileau, D. Germain, D. Thomas and F. Gossard (1990). Intracellular proteolytic processing of proopiomelanocortin in heterologous COS-1 cells by the yeast KEX2 endoprotease. *Biochem. Cell. Biol. 68*, 635–640.
14. C. Clamagirand, M. Camier, H. Boussetta, C. Fahy, A. Morel, P. Nicolas and P. Cohen (1986). An endopeptidase associated with bovine neurohypophysis secretory granules cleaves pro-ocytocin/neurophysin peptide at paired basic residues. *Biochem. Biophys. Res. Commun. 134*, 1190–1196.
15. C. Clamagirand, M. Camier, C. Fahy, C. Clavreul, C. Créminon and P. Cohen (1987). C-terminally extended oxytocin and pro-oxytocin/neurophysin peptide converting enzyme in bovine corpus luteum. *Biochem. Biophys. Res. Commun. 143*, 789–796.
16. C. Créminon, M. Rholam, H. Boussetta, N. Marrakchi and P. Cohen (1988). Synthetic peptides substrates as models to study a pro-ocytocin neurophysin converting enzyme. *J. Chromatogr. 440*, 439–448.
17. N. Brakch, H. Boussetta, M. Rholam and P. Cohen (1989). Processing endoprotease recognizes a structural feature at the cleavage site of peptide prohormones. The proocytocin/neurophysin model. *J. Biol. Chem. 264*, 15912–15916.
18. S. Gomez, G. Boileau, L. Zollinger, C. Nault, M. Rholam and P. Cohen (1989). Site specific mutagenesis identifies amino acid residues critical in prohormone processing. *EMBO J, 8*, 2911–2916.
19. M. Rholam, P. Nicolas and P. Cohen (1986). Precursor for peptides hormones share common secondary structures features at the proteolytic processing sites. *FEBS Lett. 207*, 1–6.
20. M. Rholam, P. Cohen, N. Brakch, L. Paolillo, A. Scatturin and C. Di Bello (1990). Evidence for β-turn structure in model peptides reproducing pro-ocytocin/neurophysin proteolytic processing site. *Biochem. Biophys. Res. Commun. 168*, 1066–1073.
21. L. Paolillo, M. Simonetti, N. Brakch, G. D'Auria, M. Saviano, M. Dettin, M. Rholam, A. Scatturin, C. Di Bello and P. Cohen (1992). Evidence for the presence of a secondary structure at the dibasic processing site of prohormone: the pro-ocytocin model. *EMBO J, 11*, 2399–2405.
22. G. A. Grant: *Synthetic Peptides*, UNBC Biotechnical Resource Series, Freeman, New York 1992.
23. U. Piantini, O. W. Sørensen and R. R. Ernst (1982). Multiple quantum filters for elucidating NMR coupling networks. *J. Am. Chem. Soc. 104*, 6800–6801.
24. A. Bax and D. G. Davis (1985). MLEV-17-based two-dimensional homonuclear magnetization transfer spectroscopy. *J. Magn. Res. 65*, 355–360.
25. D. Neuhaus and M. Williamson: *The Nuclear Overhauser Effect*, VCH Publishers, New York 1989.
26. A. A. Bothner-By, R. L. Stephens, J. Lee, C. D. Warren and R. Jeanloz (1984). Structure determination of a tetrasaccharide: transient nuclear Overhauser effect in the rotating frame. *J. Am. Chem. Soc. 106*, 811–813.
27. S. Lifson, A. T. Hagler and P. Dauber (1979). Consistent force field studies of intermolecular forces in hydrogen-bonded crystal. 1. Carboxylic acids, amides, and the C=O H hydrogen bonds. *J. Am. Chem. Soc. 101*, 5111–5121.
28. S. Lifson, A. T. Hagler and P. Dauber (1979). Consistent force field studies of intermolecular forces in hydrogen-bonded crystal. 2. A benchmark for the objective comparison of alternative force fields. *J. Am. Chem. Soc, 101*, 5122–5130.
29. S. Lifson, A. T. Hagler and P. Dauber (1979). Consistent force field studies of intermolecular forces in hydrogen-bonded crystal. 3. The C=O H=O hydrogen bond and the analysis of the energetics and packing of carboxylic acids. *J. Am. Chem. Soc. 101*, 5131–5141.
30. L. Verlet (1967). Computer experiments on classical

fluids. I. Thermodynamical properties of Lennard-Jones molecules. *Phys. Rev. 159*, 98–103.
31. C. L. Brooks III, B. Montgomery Pettitt and M. Karplus (1985). Structural and energetic effect of truncating long ranged interaction in ionic and polar fluids. *J. Chem. Phys. 83*, 5897–5908.
32. C. L. Brooks III, B. Montgomery Pettitt and M. Karplus: *Proteins: A Theoretical Perspective of Dynamics, Structure and Thermodynamics*; Wiley, New York 1988.
33. R. W. Woody in: *The Peptides: Analysis, Synthesis and Biology, Vol. 7*, p. 15–114. J. Hruby Ed, Academic Press, New York 1985.
34. D. M. Byler and H. Susi (1986). Examination of the secondary structure of proteins by deconvolved FTIR spectra. *Biopolymers 25*, 469–487.
35. G. W. Bushnell, G. V. Louie and G. D. Brayer (1990). High resolution three-dimensional structure of horse heart cytocrome C. *J. Mol. Biol. 214*, 585–595.
36. A. Dong, P. Huang and W. S. Caughey (1990). Protein secondary structures in water from second derivative amide I infrared spectra. *Biochemistry 29*, 3303–3308.
37. M. Hollósi, ZS. Majer, A. Z. Rónai, A. Magyar, K. Medzihradszky, S. Holly, A. Perczel and G. D. Fasman (1994). CD and Fourier transform IR spectroscopic studies of peptides. II. Detection of β-turns in linear peptides. *Biopolymers 34*, 177–185.
38. W. K. Surewicz, H. H. Mantsch and D. Chapman (1993). Determination of protein secondary structure by Fourier transform infrared spectroscopy: a critical assessment. *Biochemistry 32*, 388–394.
39. H. H. Mantsch, A. Perczel, M. Hollósi and G. D. Fasman (1993). Characterization of β-turns in cyclic hexapeptides in solution by Fourier transform IR spectroscopy. *Biopolymers 33*, 201–207.
40. S. Yu, Venyaminov and N. N. Kalnin (1990). Quantitative IR spectroscopy of peptide compounds in water (H_2O) solutions. I. Spectral parameters of amino acid residue absorption bands. *Biopolymers 30*, 1243–1257.
41. Yu. N. Chirgadze, O. V. Feodorov and N. P. Trushina (1975). Estimation of amino acid residue side-chain absorption in infrared spectra of protein solutions in heavy water. *Biopolymers 14*, 679–694.
42. K. Wütrich: *NMR of Proteins and Nucleic Acids*. Wiley, New York 1986.
43. H. J. Tracy and R. A. Gregory (1964). Physiological properties of a series of synthetic peptides structurally related to gastrin. *Nature 204*, 935–938.
44. J. E. Rivier and M. R. Brown (1978). Bonbesin, bonbesin analogues, and related peptides: effect on thermoregulation. *Biochemistry 17*, 1766–1771.
45. M. Mutter and R. Hersperger (1990). Peptides as conformational switch: medium-induced conformational transitions of designed peptides. *Angew. Chem. Int. Ed. Eng. 29*, 185–187.
46. G. D. Fasman: *Poly-α-Amino Acids*, p. 499–604. G. D. Fasman Ed., Dekker, New York 1967.
47. M. Jackson and H. H. Mantsch (1991). Beware of proteins in DMSO. *Biochim. Biophys. Acta 1078*, 231–235.
48. J. Baudekar (1992). Amide modes and protein conformation. *Biochim. Biophys. Acta 1120*, 123–143.
49. A. Motta, D. Picone, T. Tancredi and P. A. Temussi (1987). NOE measurements in linear peptides in cryoprotective aqueous mixtures. *J. Magn. Res. 75*, 364–370.
50. W. S. Sossin, J. M. Fisher and R. H. Scheller (1990). Sorting within the regulated secretory pathway occurs in the trans-Golgi network. *J. Cell Biol. 110*, 1–12.
51. E. Schnabel, R. E. Mains and M. G Farquhar (1989). Proteolytic processing of pro-ACTH/endorphin begins in the Golgi complex of pituitary corticotrophs and AtT-20 cells. *Mol. Endocrinol. 3*, 1223–1235.
52. A. Lepage-Lezin, P. Jopseph-Bravo, G. Devilliers, L. Benedetti, J.-M. Launay, S. Gomez and P. Cohen (1991). Prosomatostatine is processed in the Golgi apparatus of rat neural cells. *J. Biol. Chem. 266*, 1679–1688.